Plasmonics (2022) 17:213–222
https://doi.org/10.1007/s11468-021-01507-5

Platinum Layers Sandwiched Between Black Phosphorous and Graphene for Enhanced SPR Sensor Performance

Maheswari Pandaram[1] · Subanya Santhanakumar[2] · Ravi Veeran[1] · Rajesh Karuppaiya Balasundaram[3] · Rajan Jha[4] · Zbigniew Jaroszewicz[5,6]

Received: 20 May 2021 / Accepted: 26 July 2021 / Published online: 6 August 2021

Abstract

Highly sensitive surface plasmon resonance (SPR) sensor consisting of Ag-Pt bimetallic films sandwiched with 2D materials black phosphorus (BP) and graphene over Pt layer in Kretschmann configuration is analyzed theoretically using the transfer matrix method. Numerical results show that upon suitable optimization of thickness of Ag-Pt layers and the number of layers of BP and graphene, sensitivity as high as 412°/RIU (degree/refractive index unit) can be achieved for p-polarized light of wavelength 633 nm. This performance can be tuned and controlled by changing the number of layers of BP and graphene. Furthermore, the addition of graphene and heterostructures of black phosphorus not only improved the sensitivity of the sensor but also kept the FWHM of the resonance curve much smaller than the conventional sensor utilizing Au as plasmonic metal and hence improved the resolution to a significant extent. We expect that this new proposed design will be useful for medical diagnosis, biomolecular detection, and chemical examination.

Keywords Surface plasmon · Sensitivity · Black phosphorous · Platinum · Graphene

Introduction

Surface plasmon resonance (SPR) is the one of the most powerful optical techniques used for medical diagnostics, enzyme and gaseous detection, and food safety [1–8]. This technique has been widely used for a quick and accurate detection of various physical and biochemical parameters. Most of the SPR-based sensor uses Kretschmann's attenuated total reflection (ATR) method, in which the p-polarized incident light excites a surface plasmon wave (SPW) along the metal–dielectric interface on the thin metallic layer deposited on the base of an optical coupling prism [9]. The choice of metallic film is one of the crucial aspects in designing SPR-based applications. Usually gold (Au) is considered as the most suitable plasmonic material as it is highly resistive to oxidization, possesses better chemical stability, and provides higher sensitivity. Silver, on the other hand, shows better resolution whereas it oxidizes easily and possesses lesser sensitivity compared to Au. The bimetallic configuration of Au/Ag utilizes the advantages of both the metals and has been demonstrated in several works. It is noted that the usage of bimetallic film, though it improved the resolution of the sensor, its sensitivity seems not much improved [10–13]. Apart from Au and Ag, more metals have been identified for SPR sensing such as aluminum (Al), nickel (Ni), copper (Cu), and platinum (Pt), and each of these metals has their own advantages and disadvantages [14–16]. Recently, platinum has been identified as a potential SPR-active metal owing to its strong dependence of reflection coefficient on wavelength in the visible region of the spectrum, high reflecting property, inert, chemically stable with high melting point, and prolonged stability [17–19]. Shukla et al. theoretically

✉ Rajesh Karuppaiya Balasundaram
rajeskb@gmail.com

1 Department of Physics, Government Arts College, Salem-636007, Tamil Nadu, India

2 Department of Physics, PSGR Krishnammal College for Women, Coimbatore, Tamil Nadu, India

3 Department of Physics, Chikkanna Government Arts College, Tirupur, Tamil Nadu, India

4 Nanophotonics and Plasmonics Laboratory, School of Basic Sciences, IIT, Bhubaneswar 752050, Odisha, India

5 Department of Physical Optics, Institute of Applied Optics, Warsaw, Poland

6 National Institute of Telecommunications, Warsaw, Poland

analyzed the performance of the SPR sensor with platinum layer coated on optical fiber. They observed that the sensitivity of the sensor enhances linearly with the increase in the refractive index of the sensing medium for all thickness of platinum layer and for a given refractive index of the sensing medium [20]. Recently, black phosphorus (BP) is identified as one of the potential 2D materials [21] which gain rapid attention due to its widely tunable and direct bad gap, remarkable electrical and optical properties, and higher carrier mobility [22–25]. The BP also provides attractive physical, chemical, and mechanical anisotropic properties which make it a suitable candidate for high performance potential and chemical applications [26]. Srivastava et al. reported that implementation of double layer BP enhanced the sensitivity by 35% [27]. Recently, graphene, on the other hand, exhibits remarkable properties such as high charge carrier mobility which induces strong coupling at the interface between metal-graphene films [28]. Wu et al. reported that utilizing graphene layers enhanced the sensitivity by 25% compared with conventional gold–based SPR sensor [29]. Recently, many studies on enhancement of sensitivity of the SPR sensor upon utilizing graphene layers are attempted from numerical aspects [5, 30]. Furthermore, graphene is impermeable to gases such as oxygen and helium because the electron density of hexagonal rings is enough to prevent atoms and molecules from passing through the ring structure [31]. Hence, graphene can be used as a protective layer against oxidation of metals which is also found to improve the sensitivity of the sensor to a great extent [32]. Recently, SPR biosensors based on Blue P-TMDC-graphene heterostructure [33] and graphene-$BaTiO_3$ nanosheets [34] have also been proposed.

In this paper, we have designed a new sensor configuration composed of Ag-Pt bi-metallic films sandwiched with 2D materials BP and graphene over Pt layer. Here, we report that ultra-high sensitivity of the SPR sensor can be realized upon suitable optimization of thickness of metal layers and no. of layers of BP and graphene. Here, it is noted that the proposed sensing configuration not only enhances sensitivity but also still keeps the FWHM of the resonance curve much smaller than the conventional sensor utilizing Au as plasmonic material and hence improved the resolution to a greater extent. Moreover, the top surface graphene coat not only protected the metal surface but also improved the biomolecular absorption through high surface to volume ratio and Pi conjugation structure.

Theory

The structure of the proposed SPR biosensor is given in Fig. 1 which consists of a multilayer (six layers) structure. Keeping in mind the widely used prism required

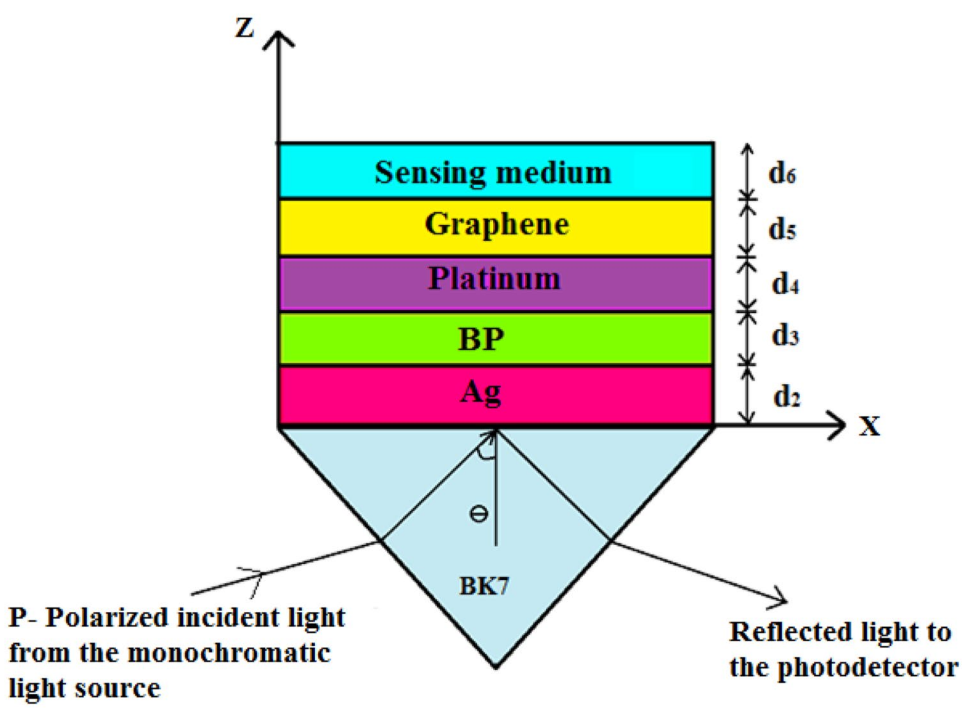

Fig. 1 Schematic diagram of the proposed SPR biosensor

for momentum match, the first layer is of BK7 prism. The second layer is an optimized thickness of 40-nm thickness of silver which is deposited on the base of the coupling prism. The third and fourth layers are BP and 15-nm thickness of platinum. The fifth layer is considered as graphene followed by a sensing layer. TM-polarized light, wavelength of 633 nm, is used at one face of the prism and is assumed to be collected from the other face with proper optics. The dispersion of prism is considered as [35]

$$n_{\mathrm{BK7}} = \left(\frac{1.03961212\lambda^2}{\lambda^2 - 0.00600069867} + \frac{0.231792344\lambda^2}{\lambda^2 - 0.0200179144} + \frac{1.03961212\lambda^2}{\lambda^2 - 103.560653} + 1 \right)^{1/2} \quad (1)$$

where λ is the wavelength of incident light in micrometers.

The wavelength dependence dielectric constant of silver is calculated using Drude-Lorentz formula, given by

$$\varepsilon_m(\lambda) = \varepsilon_{mr} + \varepsilon_{mi} = 1 - \frac{\lambda^2 \lambda_c}{\lambda_p^2(\lambda_c + i\lambda)} \quad (2)$$

where $\lambda_p = 1.4541 \times 10^{-7}$ m and $\lambda_c = 1.7614 \times 10^{-5}$ m. Here, λ_p and λ_c are the plasma and collision wavelength of silver (Ag), respectively [32]. The third layer is BP whose refractive index is $n_3 = 3.5 + 0.01i$ at $\lambda = 633$ nm, and the thickness of BP is calculated as $d_3 = V \times 0.53$ nm [36], where the number of BP layer is indicated by V. The fourth layer is platinum (Pt) layer, and its dielectric constant is calculated according to the Drude model as given in Eq. (3), with $\lambda_p = 2.415 \times 10^{-7}$ m and $\lambda_c = 1.795 \times 10^{-5}$ m [37]. The fifth layer is made of graphene, and its refractive index (n_5) is calculated as

$$n_5 = 3.0 + i\frac{C_1}{3}\lambda \quad (3)$$

where the constant $C_1 \approx 5.446 \mu\mathrm{m}^{-1}$ [38].

The sixth layer is the sensing medium whose refractive index is assumed to change in the range of 1.33 to 1.35 as such a change is usually attributed for the detection of biomolecules. In order to theoretically evaluate the amplitude of the reflection coefficient for p-polarized incident beam for the system with multilayer structure stacked along the z-axis, several methods including N-layer matrix method [39, 40], admittance loci method [41], and S matrix method [42] are proposed. As the N-layer matrix method is very accurate as it contains no approximation, here, we proposed to use the N-layer matrix method to evaluate the performance of the proposed sensor configuration, and such method has also been adopted for similar SPR sensor configuration proposed recently [43]. In the N-layer matrix method, the tangential fields at the boundary $Z = Z_1 = 0$ are related to those at the final boundary $Z = Z_{N-1}$ by

$$\begin{bmatrix} U_1 \\ V_1 \end{bmatrix} = M \begin{bmatrix} U_{N-1} \\ V_{N-1} \end{bmatrix} \quad (4)$$

where U_1, and V_1 are the tangential components of the magnetic and electric fields of the first layer, and U_{N-1} and V_{N-1} are the tangential components of the magnetic and electric fields of the Nth layer. M is the characteristic matrix for the proposed structure and for p-polarized light; it is given by

$$M = \prod_{k=2}^{N-1} M_k = \begin{bmatrix} M_{11} & M_{12} \\ M_{21} & M_{22} \end{bmatrix} \quad (5)$$

with

$$M_k = \begin{bmatrix} \cos\beta_k & \frac{-i\sin\beta_k}{q_k} \\ -iq_k \sin\beta_k & \cos\beta_k \end{bmatrix} \quad (6)$$

where

$$q_k = \left(\frac{\mu_k}{\varepsilon_k}\right)^{1/2} \cos\theta_k = \frac{\left(\varepsilon_k - n_1^2 \sin^2\theta_1\right)^{1/2}}{\varepsilon_k}$$

and

$$\beta_k = \frac{2\pi}{\lambda} n_k \cos\theta_k \left(z_k - z_{k-1}\right) = \frac{2\pi d_k}{\lambda}\left(\varepsilon_k - n_1^2 \sin^2\theta_1\right)^{1/2}$$

Here, θ and λ represent angle and wavelength of the incident light. The proposed model consists of six layers, and hence, $N = 6$. Thus, transfer matrices are calculated in accordance with Eq. (6), and the corresponding amplitude reflection coefficient (r_p) is given as

$$r_p = \frac{\left(M_{11} + M_{12}q_N\right)q_1 - \left(M_{21} + M_{22}q_N\right)}{\left(M_{11} + M_{12}q_N\right)q_1 + \left(M_{21} + M_{22}q_N\right)} \quad (7)$$

In the above equation, q_1 and q_{N} correspond to the BK7 substrate and the sensing layer, respectively, and finally, the reflectivity (R_p) can be given as

$$R_p = \left|r_p\right|^2 \quad (8)$$

Sensitivity of the SPR biosensor is measured as the small change in the refractive index $\left(\Delta n_s\right)$ of the analyte with the change in resonance condition in the reflectance curve ($\Delta\theta_{\mathrm{res}}$); therefore, the sensitivity is given by

$$S = \frac{\Delta\theta_{\mathrm{res}}}{\Delta n_s} \quad (9)$$

The other prominance parameters of the SPR sensors are quality factor (Q) and signal-to-noise ratio (SNR);

these parameters should be high for the good sensors. SNR is defined as the ratio of resonance angle shift ($\Delta\theta_{res}$) and the full width at half maxima (FWHM) ($\Delta\theta_{0.5}$) of the reflectance curve,

$$SNR = \frac{\Delta\theta_{res}}{\Delta\theta_{0.5}} \tag{10}$$

The quality factor (Q) is given by

$$Q = \frac{S}{\Delta\theta_{0.5}} \tag{11}$$

where,

$S(\theta)$ — sensitivity of the SPR biosensor
$\Delta\theta_{0.5}$ — FWHM of the SPR curve

Results and Discussions

In the proposed work, we numerically analyzed the performance of the new SPR sensor configuration (Ag-BP-Pt-graphene) using the transfer matrix method. The condition of minimum reflectance (R_{min}) close to zero ensures coupling of maximum energy of incident TM polarized light with the surface plasmon, and it is necessary for the design of any SPR sensor to have improvised sensitivity and resolution [44–46]. In order to ensure such a condition, here we fixed one such possible configuration with thicknesses of Ag as 40 nm and Pt as 15 nm. Figure 2a shows the reflectance curve plotted corresponding to the change in RI (refractive index) of the sensing medium from 1.330 to 1.335 ($\Delta n_s = 0.005$) in the absence of BP and graphene ($V = 0$ and $L = 0$). As can be clearly seen from Fig. 2a that

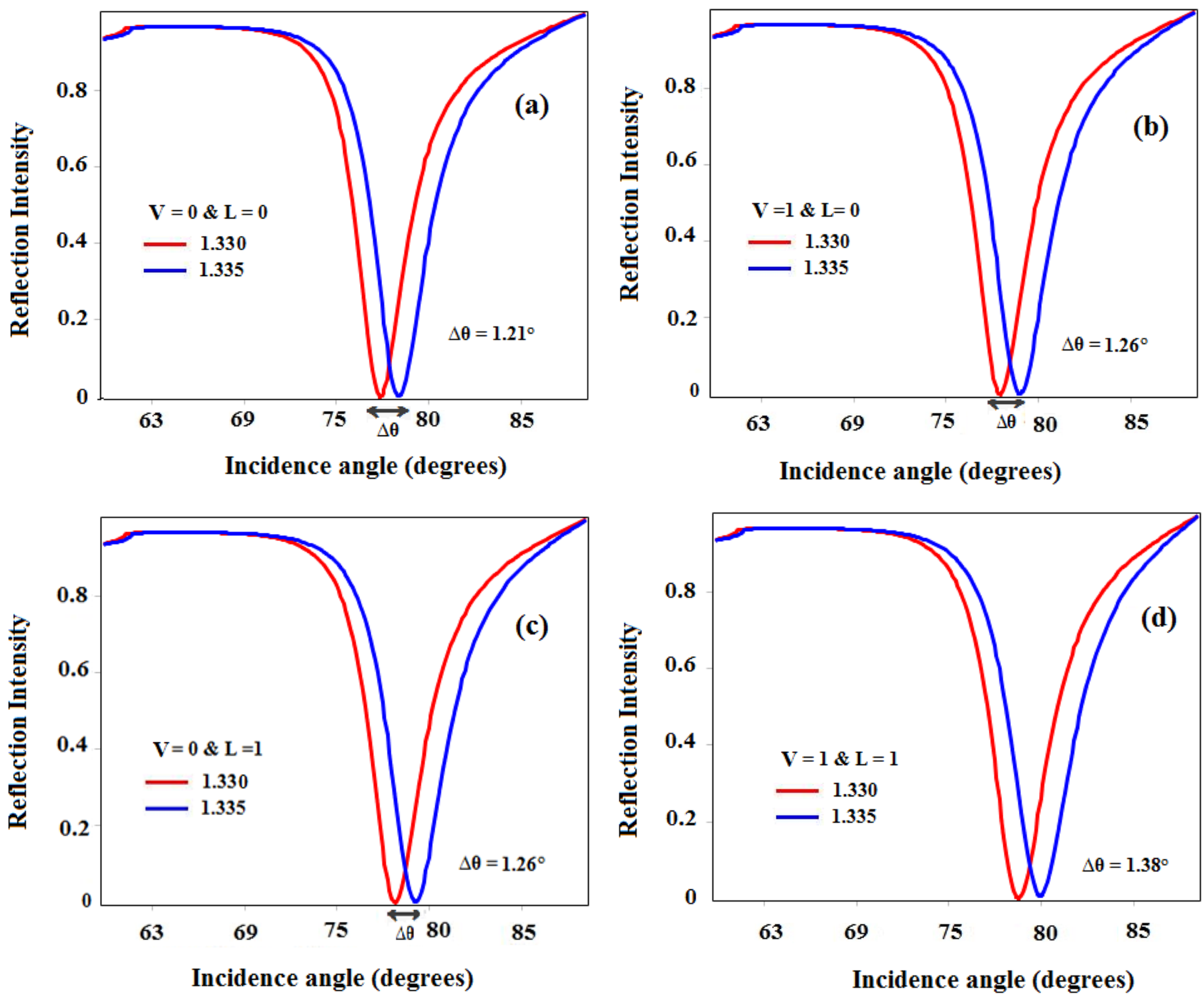

Fig. 2 Reflection intensity as a function of incident angle with **a** $V = 0$ and $L = 0$, **b** $V = 1$ and $L = 0$, **c** $V = 0$ and $L = 1$, and **d** $V = 1$ and $L = 1$

the shift in the resonance angle is measured as $\Delta\theta = 1.21°$, and the corresponding sensitivity calculated as per Eq. (9) is 240.76°/RIU. Figure 2b and c show that upon introducing a single layer of either BP or graphene ($V = 1$ and $L = 0$ or $V = 0$ and $L = 1$) improved the shift in resonance angle as $\Delta\theta = 1.26°$, and the corresponding sensitivity is calculated as 252.23°/RIU. Hence, it is to be noted that the addition of either the monolayer of graphene or BP is found to have the same effect on the sensitivity of the sensor. However, it is further noted from Fig. 2d that for the proposed sensor configuration with the inclusion of both monolayer of BP and graphene ($V = 1$ and $L = 1$), the shift in the resonance curve is found to be significantly improved as $\Delta\theta = 1.38°$ due to the different values of the dielectric constant of the materials which fulfill the resonance condition at different angles. The corresponding sensitivity is found to have much improved as 275.15°/RIU. As the sensitivity enhancement depends on the absorption of incident light in the different layers, the proposed configuration with single layers of BP and graphene shows better absorption and, hence, exhibits much improvement in the sensitivity compared with traditional structure [47].

Figure 3a shows the shift in dip of the SPR curve corresponding to the change in RI of the sensing medium in the range of 1.330 to 1.350. It is noted that, without BP and graphene ($M = 0$ and $L = 0$), the shift in the dip varies from 76.18 to 81.0°, whereas it increased from 76.75 to 82.4° for the configuration with the inclusion of the monolayer of BP ($V = 1$ and $L = 0$) which is due to a strong dispersion of BP around the incident wavelength. It is also noted that further increases in $\Delta\theta$ around 76.96 to 82.4° are obtained for the configuration with the monolayer of graphene ($V = 0$ and $L = 1$) which shows better absorption property of graphene over BP. However, for the configuration with the inclusion of both BP and graphene ($V = 1$ and $L = 1$) layers, the shift in the resonance curve dip is found to have improved very much from 78.65 to 85.58° which is due to the combined effect of both the layers. Figure 3b shows the variation of sensitivity of the proposed sensor with respect to the refractive index of the sensing medium by keeping the other parameter the same as before. We observed that for the configuration without BP and graphene layers, the sensitivity increased from 206.29 to 332.48°/RIU ($V = 0$ and $L = 0$). However, in the inclusion of BP ($V = 1$ and $L = 0$), the sensitivity is found to vary from 217.83 to 378.34°/RIU, whereas an addition of the monolayer of graphene without BP ($V = 0$ and $L = 1$) enhances the sensitivity from 229.29 to 389.8°/RIU. It is also noted that for the configuration considered with the inclusion of both monolayers of BP and graphene ($V = 1$ and $L = 1$), further improved the sensitivity from 252.2 to 435.6°/RIU, which is due to the combined effect of both the 2D materials as the dispersion variation is different for both BP and graphene which results in a modified

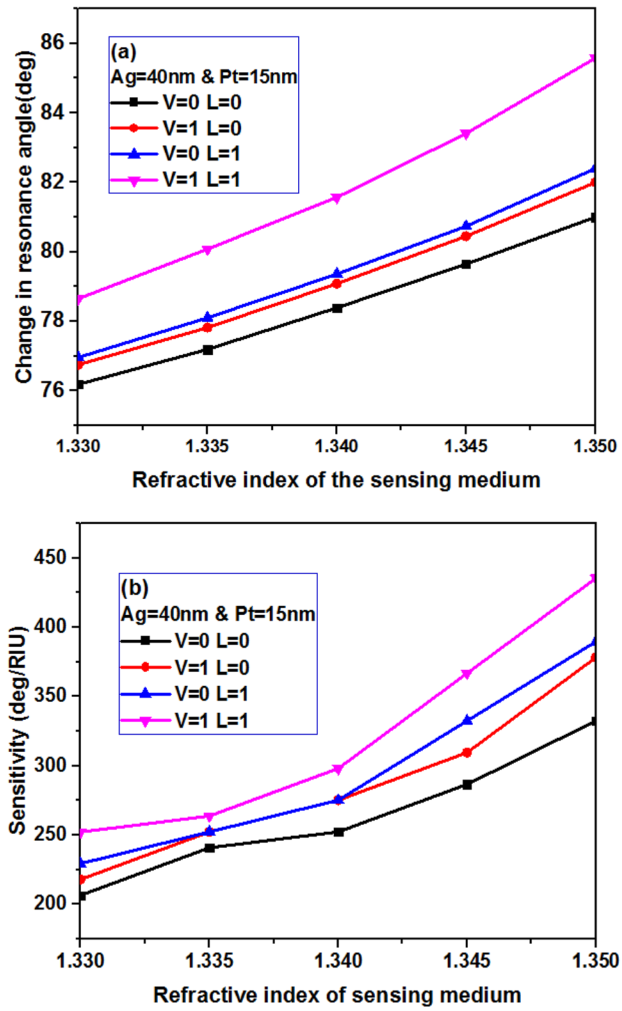

Fig. 3 **a** Change in resonance shift, **b** sensitivity corresponding to the change in RI of the sensing medium from 1.330 to 1.335

effective index around the wavelength of operation. Here, we concluded that the addition of BP and graphene layers can significantly improve the sensitivity of the proposed biosensor compared with the conventional gold–based SPR structure [47].

Furthermore, we optimized the no. of graphene and BP layers required to achieve the best performance of the proposed sensor. Figure 4a shows the reflection spectra versus the angle of incidence obtained for a monolayer of graphene with increasing number of black phosphorus (BP) layers for Ag = 40 nm and Pt = 15 nm. It is noted from Fig. 4a that the increasing number of BP layers largely shifts the reflectance dip as the resonance condition is satisfied at a higher angle and, hence, improved the sensitivity, which is due to higher mobility of charge carriers and higher absorption efficiency of BP [48]. We also observed that similar shift in resonance curve is also noted for the addition of graphene layers as shown in Fig. 4b and found to be larger than the addition of

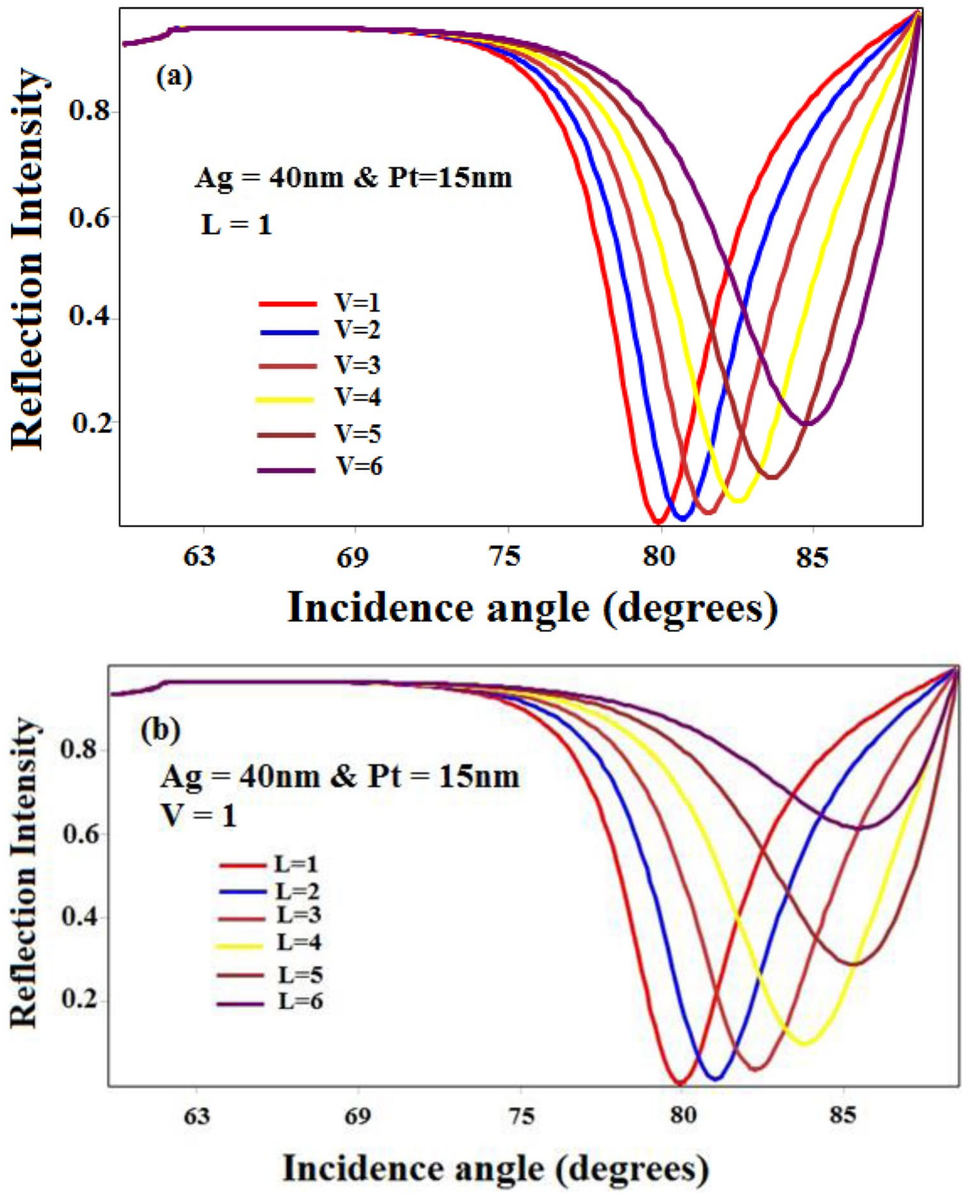

Fig. 4 Reflection intensity as the function of incident angle **a** different layers of black phosphorus (BP) with monolayers of graphene, **b** different layers of graphene with monolayer of BP

BP layers owing to the large real part of dielectric constant of graphene.

It is also noted from both Fig. 4a and b that increasing either the no. of BP and graphene layers not only generates larger shift in resonance dip but also makes the resonance curve wider and shifts the R_{min} to higher values. Such an increase in FWHM of the spectral curve is due to the decrease of the propagation velocity of SP waves in 2D materials which results in damping [49]. The increase in R_{min} is due to the saturation in absorption of incident light energy and the increase of electron loss [50–52]. It is also noted that widening of resonance curve and increase in R_{min} are higher for graphene due to its large imaginary part of dielectric constant when compared to BP. This means arbitrarily increasing either BP or graphene layers makes the SPR curve broader, and it is more difficult to measure near the resonance angle, thereby affecting the accuracy of the measurement. Thus, we can conclude that one cannot arbitrarily increase the number of BP and graphene layers as an attempt to improve the sensitivity of the sensor.

Based on the above analysis, to optimize the number of BP and graphene layers, we calculated the sensitivity for the BP and graphene layers. Figure 5 shows the minimum reflectance (R_{min}) and sensitivity corresponding to the number of graphene layers with a monolayer of BP for the configuration Ag = 40 nm and Pt = 15 nm. It is clearly observed that the sensitivity of the proposed configuration increased till increase of the number of graphene layers as four, and then it starts to decrease. This is because of increase of minimum reflectance (R_{min}) from the 4th layer onwards as it reduces the absorption

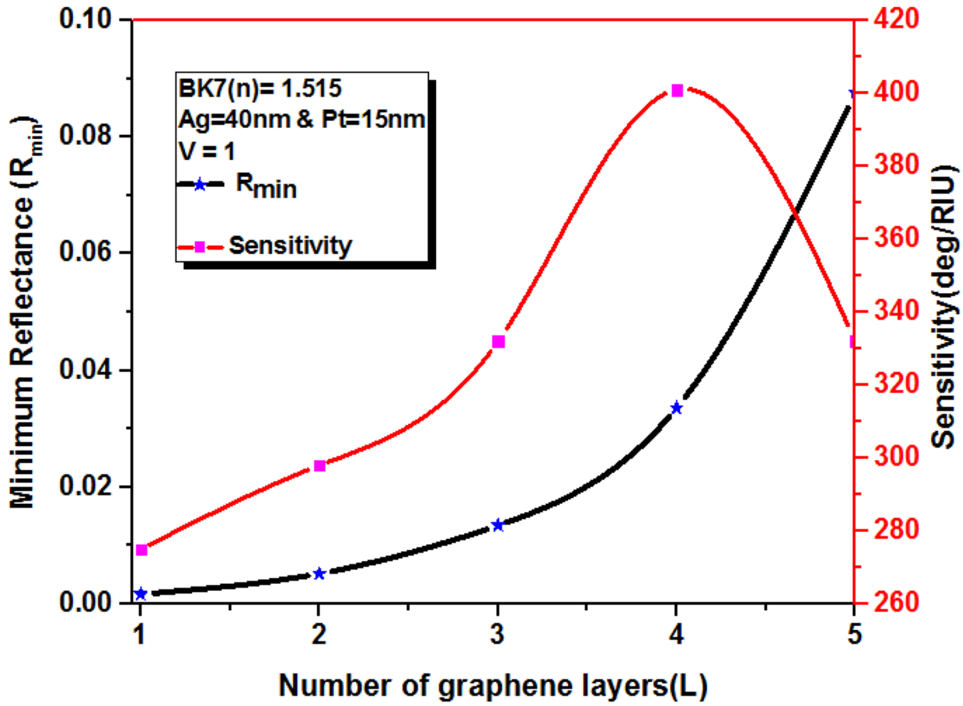

Fig. 5 Minimum reflectance and sensitivity as functions of number of graphene layers (L)

of light, i.e., optical energy losses occurred due to the increasing number of graphene layers. Hence, for the proposed configuration, we optimized the no. of graphene layers as 4 for the best performance. The R_{min} and sensitivity obtained for the optimized graphene layer ($L=4$) are 0.0336 and 401°/RIU respectively. Figure 6 shows the variation of R_{min} and sensitivity versus number of BP layers with optimized no. layers of graphene ($L=4$). From Fig. 6, it is noted that the sensitivity of the proposed sensor improved till the addition of the 2nd layer of BP, and it is found to start decreasing sharply. This suggests that we just need to choose $V=2$ for getting a maximum sensitivity for sensing applications. It is observed that after optimization of BP and graphene layers ($V=2$ and $L=4$),

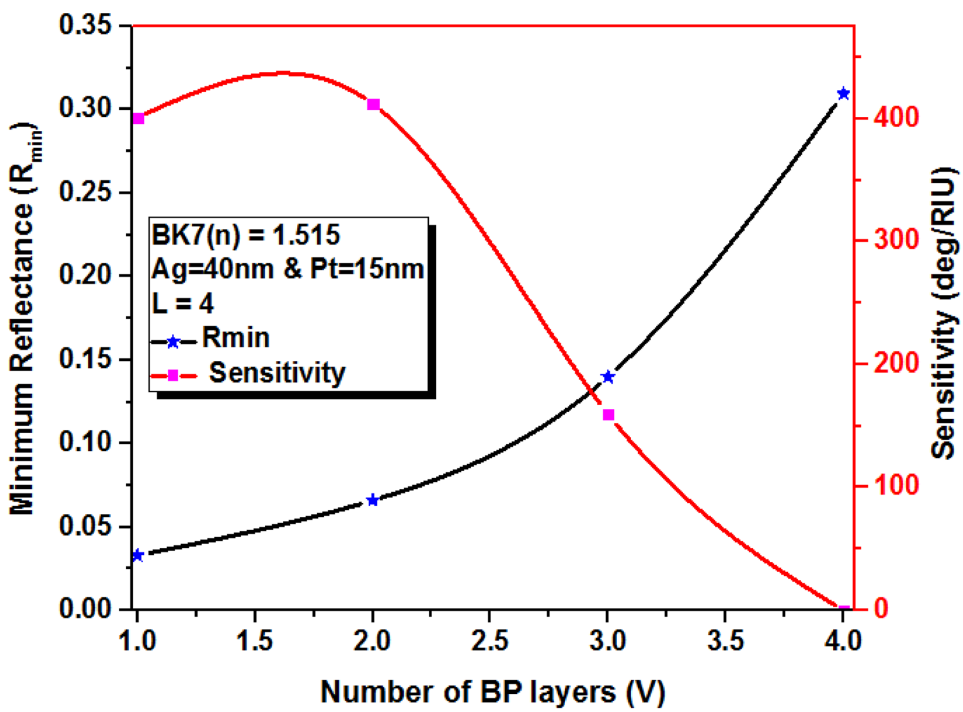

Fig. 6 Minimum reflectance and sensitivity as a function of number of BP layers (V)

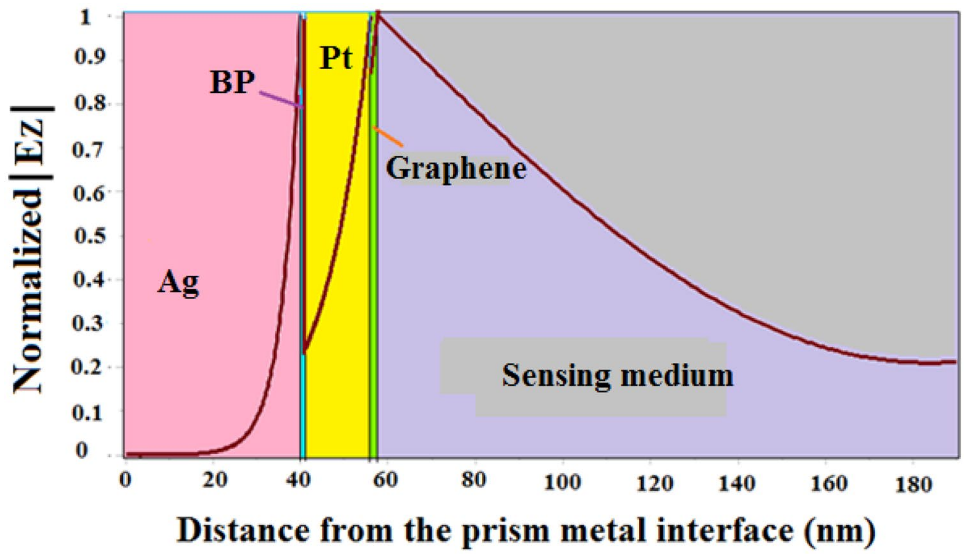

Fig. 7 Normalized electric field distribution of SP wave in the proposed SPR sensor

the sensitivity of the proposed biosensor improved very much as 412°/RIU and can still keep the FWHM value as 5.731°. The signal-to-noise ratio (SNR) and quality factor (Q) are calculated using Eqs. (10–11) and are found to be as $0.36^{\circ -1}$ and 71.88 RIU^{-1}, respectively. Furthermore, to have a better insight into the electric field distribution at different layers in the proposed multilayered system, the normalized electric field distribution of SP wave at different layers is plotted and is shown in Fig. 7. It is noted from Fig. 7 that the Ag layer enhances the electric field and shows a peak at the Ag-BP interface. The field intensity falls in the BP layers and further gets much enhanced in the platinum (Pt) layer which shows the excitation of SPs at this interface. It is noted that an addition of graphene layer further increases the field intensity which reaches its maximum at the interface of the graphene-sensing medium and decays exponentially in the sensing medium. This enhanced probing field close to the graphene layer with long probing depth is highly sensitive to biomolecular interaction throughout the penetrating depth. Such an enhanced probing evanescent field increases the interaction volume and hence maximize the sensitivity of the sensor [40, 53].

Finally, we concluded that the proposed sensor with the configuration of 40-nm thickness of Ag, with two layers of BP, 10 nm of platinum (Pt), and four layers of graphene over Pt can enhance the sensitivity as high as 412°/RIU with FWHM of 5.731°. The signal-to-noise ratio and quality factor values are noted as $0.36^{\circ -1}$ and 71.88 RIU^{-1}, respectively. The FWHM obtained here is nearly close to the Au–Ag bimetallic film–based SPR sensor; however, the sensitivity achieved is found to be much higher [54]. Some of the relevant works and its sensitivity have been compared in Table 1. We expect on the basis of the enhanced performance of sensitivity and lower FWHM of the SPR curve, the proposed sensor will have better performance in the chemical and biological applications.

Table 1 Comparison among proposed biosensors with other existing biosensors

S. no	Configuration	Sensitivity (°/RIU)	Reference
1	Prism/Au/graphene/affinity layer/sensing layer	47.43	[55]
2	Prism/Au/graphene/MoS_2/PBS solution	87.8	[56]
3	Prism/few layer BP film/graphene/PBS solution	125	[57]
4	Prism/chromium/Au/BP/2D material	187	[32]
5	Prism/air gap/Ag/ITO/MoS_2/graphene	189	[48]
6	Prism/Ag/WS_2/Ni/graphene/sensing medium	243.31	[58]
7	Prism/Ag/Si/BP/Mxene	264	[43]
8	Prism/Ag/BP/WSe_2	279	[36]
9	Prism-air-WS_2-Al-WS_2-graphene	315.52	[51]
10	Prism/Ag/BP/Pt/graphene/sensing medium	412	Proposed work

Conclusion

In this paper, we theoretically proposed an SPR sensor configuration sandwiching BP layers between silver- and graphene-coated platinum in the Kretschmann setup. We observed that, by properly optimizing the structure of the sensor, sensitivity can be enhanced as high as 412°/RIU and can still keep the FWHM of the resonance curve as small as 5.731°. We also noted that the sensitivity can be tuned and controlled by changing the number of layers of BP and graphene. We expect that such a proposed configuration exhibiting enhanced sensitivity and lower FWHM will find potential applications in food safety, chemical examination, and biological detection.

Author Contribution Maheswari Pandaram — conceptualization, data curation, and original draft preparation. Subanya Santhanakumar — software and validation. Ravi Veeran — reviewing and editing. Rajesh Karuppaiya Balasundaram — supervision and writing — reviewing and Editing. Rajan Jha — reviewing and editing. Zbigniew Jaroszewicz — reviewing and editing.

Availability of Data and Material Data and material will be made available on reasonable request.

Code Availability Code will be made available on reasonable request.

Declarations

Conflict of Interest The authors declare no competing interests.

References

1. Liedberg B, Nylander C, Sundstrom I (1983) Surface plasmon resonance for gas detection and biosensing. Sens Actuators B 4:299–304
2. Jorgenson RC, Yee SS (1993) A fiber-optic chemical sensor based on surface plasmon resonance. Sens Actuators B 12:213–220
3. Wang TJ, Tu CW, Liu FK, Chen HL (2004) Surface plasmon resonance waveguide biosensor by bipolarization wavelength interrogation. IEEE Photonics Technol Lett 16:1715–1717
4. Srivastava T, Purkayastha A, Jha R (2016) Graphene based surface plasmon resonance gas sensor for terahertz. Opt Quant Electron 48(6):334
5. Choi SH, Kim YL, Byun KM (2011) Graphene-on-silver substrates for sensitive surface plasmon resonance imaging biosensors. Opt Express 19:458–466
6. Nayak JK, Jha R (2018) Graphene-oxide coated Ag-island based inline LSPR fiber sensor. Photon Technol Lett 30(19):1667–1670
7. Nayak JK, Parhi P, Jha R (2016) Experimental and theoretical studies on localized surface plasmon resonance based fiber optic sensor using graphene oxide coated silver nanoparticles. J Phys D Appl Phys 49:285101
8. Srivastava T, Das R, Jha R (2011) Highly accurate and sensitive surface plasmon resonance sensor based on channel photonic crystal wave guides. Sens Actuators B 57:246–252
9. Kretschmann E, Reather H (1968) Radiative decay of non-radiative surface plasmons excited by light. Zeitschrift fur Nature forschung 23:2135–2221
10. Maharana PK, Bhardwaj S, Jha R (2013) Electric field enhancement in surface plasmon resonance bimettalic configuration based on chalcogenide prism. J Appl Phys 114:014304–014314
11. Wang Y, Meng S, Liang Y, Li L, Peng W (2013) Fiber optic surface plasmon resonance sensor with multi-alternating metal layers for biological measurement. Photonic Sensors 3:202–207
12. Jha R, Sharma AK (2009) Chalcogenide glass prism based SPR sensor with Ag–Au bimetallic nanoparticle alloy in infrared wavelength region. J Opt A: Pure Appl Opt 11:045502
13. Shalabney A, Abdulhalim I (2011) Sensitivity-enhancement methods for surface plasmon sensors. Laser Photonics Rev 5:571–606
14. Vibisha GA, Nayak JK, Maheswari P, Priyadharsini N, Nisha A, Jaroszewicz Z, Jha R (2020) Sensitivity enhancement of surface plasmon resonance sensor using hybrid configuration of 2D materials over bimetallic layer of Cu-Ni. Optics Comm 463:125337
15. Oliveira LC, Moreira CS, Neff H, Lima AM (2016) Optical properties and instrumental performance of thin noble metal (Cu, Au, Ag) films near the surface plasmon resonance. Procedia Eng 168:834–837
16. Maurya JB, Prajapati YK (2016) A comparative study of different metal and prism in the surface plasmon resonance biosensor having MoS_2-graphene. Opt Quant Electron 48(5):1–12
17. Velichkina LM, Pestryakov AN, Vosmerikov AV, Tuzovskaya IV, Bogdanchikova NE, Avalos M, Farias M, Tiznado H (2008) Catalytic activity in hydrocarbon conversion of pentasil containing platinum, nickel, iron, or zinc nanoparticles. Pet Chem 48:201–205
18. Velichkina LM, Pestryakov AN, Vosmerikov AV, Tuzovskaya IV, Bogdanchikova NE, Avalos M, Farias M, Tiznado H (2008) Catalytic activity in the hydrocarbon conversion of system containing platinum, nickel, iron, or zinc nanoparticles. Pet Chem 48:355–359
19. Chen A, Holt-Hindle P (2010) Platinum based nanostructured materials, synthesis, properties, and applications. Chem Rev 110:3767–3804
20. Shukla S, Rani M, Sharma MK, Sajal V (2015) Sensitivity enhancement of surface plasmon resonance based fiber optic sensor utilizing platinum layer. Optik 126:4636–4639
21. Churchill HO, Jarilloherrero P (2014) Two-dimensional crystals: phosphorus joins the family. Nat Nanotechnol 9(5):330–331
22. Li L, Yu Y, Ye GL, Ge Q, Ou X, Wu H, Feng D, Chen XH, Zhang Y (2014) Black phosphorus field-effect transistors. Nat Nanotechnol 9(5):372–377
23. Qiao J, Kong X, Hu ZX, Yang F, Ji W (2014) High-mobility transport anisotropy and linear dichroism in few-layer black phosphorus. Nat Commun 5:4475
24. Rodin AS, Carvalho A, Castro Neto AH (2014) Strain-induced gap modification in black phosphorus. Phys Rev Lett 112(17):176801–176801
25. Wang X, Jones AM, Seyler KL, Tran V, Jia Y, Zhao H, Wang H, Yang L, Xu X, Xia F (2014) Highly anisotropic and robust excitons in monolayer black phosphorus. Nat Nanotechnol 10(6):517–521
26. Mao N et al (2016) Optical anisotropy of BP in the visible regime. J Am Chem Soc 138(1):300–305
27. Srivastava T, Jha R (2018) Black phosphorus: a new platform for gaseous sensing based on surface plasmon resonance. IEEE 99:1–1
28. Elias DC, Gorbachev RV, Mayorov AS, Morozov SV, Zhukov AA, Blake P, Ponomarenko LA, Grigorieva IV, Novoselov KS, Guinea F, Geim AK (2011) Dirac cones reshaped by interaction effects in suspended graphene. Nat Phys 7:701–704

29. Wu L, Chu HS, Koh WS, Li EP (2010) Highly sensitive graphene biosensors based on surface plasmon resonance. Opt Express 18:14395–14400
30. Nayak JK, Maharana PK, Jha R (2017) Dielectric over-layer assisted graphene, its oxide and MoS_2 based fibre optic sensor with high field enhancement. J Phys D Appl Phys 50:405112
31. Jiang DE, Cooper VR, Dai S (2009) Porous graphene as the ultimate membrane for gas separation. Nano Letter 9(12):4019–4024
32. Meshginqalam B, Barvestani J (2018) Performance enhancement of SPR biosensor based on phosphorene and transition metal dichalcogenides for sensing DNA hybridization. IEEE Sens J 18:7537–7543
33. Han L, Zhimin Hu, Pan J, Huang T, Luo D (2020) High sensitivity Goos-Hanchen shifts sensor based on Blue P-TMDC-graphene heterostructure. Sensors 20(12):3605
34. Pal A, Jha A (2021) A theoretical analysis on sensitivity improvement of an SPR refractive index sensor with graphene and $BaTiO_3$ nanosheets. Optik 231:166378
35. Lin Z, Jiang L, Wu L, Guo J, Dai X, Xiang Y, Fan D (2016) Tuning and sensitivity enhancement of surface plasmon resonance biosensor with graphene covered Au-MoS_2-Au films. IEEE Photonics J 8(6):4803308
36. Leiming Wu, Guo J, Wang Q, Shunbin Lu, Dai X, Xiang Y, FanSZU D (2017) Sensitivity enhancement by using few-layer black phosphorus-graphene/TMDCs heterostructure in surface plasmon resonance biochemical sensor. Sens Actuators B 249:542–548
37. Ordal MA, Bell RJ, Alexander RW Jr, Long LL, Querry MR (1985) Optical properties of fourteen metals in the infrared and far infrared: Al Co, Cu, Au, Fe, Pb, Mo, Ni, Pd, Pt, Ag, Ti, V, and W. Appl Opt 24:4493–4499
38. Nayak JK, Jha R (2017) Numerical simulation on the performance analysis of a graphene coated optical fiber plasmonic sensor at anti-crossing. Appl Opt 56(12):3510–3517
39. Verma R, Gupta BD, Jha R (2011) Sensitivity enhancement of a surface plasmon resonance based biomolecules sensor using graphene and silicon layers. Sens Actuators B 160:623–631
40. Maurya JB, Prajapati YK, Singh V, Saini JP (2015) Sensitivity enhancement of surface plasmon resonance sensor based on graphene-MoS_2 hybrid structure with TiO_2-SiO_2 composite layer. Appl Phys A 121:525–533
41. Brahmachari K, Ray M (2013) Effect of prism material on design of surface plasmon resonance sensor by admittance loci method. Front Optoelectron 6(2):185–193
42. Barchiesi D (2013) Improved methods based on S matrix for the optimization of SPR biosensors. Optics comm 286:23–29
43. Kumar R, Pal S, Verma A, Prajapati YK, Saini JP (2020) Effect of silicon on sensitivity of SPR biosensor using hybrid nanostructure of black phosphorus and MXene. Super lattices and Microstructures 145:106591
44. Tiwari K, Sharma SC, Hozhabri N (2015) High performance surface plasmon sensors: simulations and measurements. J Appl Phys 118(9):093105
45. Maharana PK, Padhy P, Jha R (2013) On the field enhancement and performance of an ultra stable SPR biosensor based on graphene. IEEE Photonics Technol Lett 25(22):2156–2159
46. Srivastava JR (2020) Plexcitonic nose based on an organic semiconductor. Appl Phys Lett 117(9):093301
47. Mishra AK, Mishra SK, Verma RK (2015) An SPR-based sensor with an extremely large dynamic range of refractive index measurements in the visible region. J Phys D ApplPhys 48(43):435502
48. Han L, Chen Z, Huang T, Ding H, Chuan Wu (2019) Sensitivity enhancement of Ag-ITO-TMDCs-graphene nanostructure based on surface plasmon resonance biosensors. Plasmonics 15:693–701
49. Maharana PK, Srivastava T, Jha R (2014) Low index dielectric mediated surface plasmon resonance sensor based on graphene for near infrared measurements. J Phys D Appl Phys 47:385102
50. Zeng S, Hu S, Xia J, Anderson T, Dinh XQ, Meng XM, Coquet P, Yong KT (2015) Graphene–MoS_2 hybrid nanostructures enhanced surface plasmon resonance biosensors. Sens Actuators B Chem 207:801–810
51. Zhao X, Huang T, Ping PS, Wu X, Huang P, Pan J, Wu Y, Cheng Z (2018) Sensitivity enhancement in surface plasmon resonance biochemical sensor based on transition metal dichalcogenides/graphene heterostructure. Sensors 18(7):2056
52. Ouyang Q, Zeng S, Dinh XQ, Coquet P, Youg KT (2016) Sensitivity enhancement of MoS_2 nanosheet based surface plasmon resonance biosensor. Procedia Eng 140:134–139
53. Shalabney A, Abdulhalim I (2010) Electromagnetic fields distribution in multilayer thin film structures and the origin of sensitivity enhancement in surface plasmon resonance sensors. Sen Actuators A 159:24–32
54. Wang M, Huo Y, Jiang Z, Zhang C, Yang C, Ning T, Liu Z, Li C, Zhanga W, Mana B (2017) Theoretical design of a surface plasmon resonance sensor with high sensitivity and high resolution based on graphene–WS_2 hybrid nanostructures and Au–Ag bimetallic film. RSC Adv 7:47177
55. Maurya JB, Prajapati YK, Singh V, Saini JP, Tripathi R (2016) Improved performance of the surface plasmon resonance biosensor based on graphene or MoS_2 using silicon. Opt Commun 359:426–434
56. Rahman M, Anower M, Hasan M, Hossain M, Haque M (2017) Design and numerical analysis of highly sensitive Au-MoS_2-graphene based hybrid surface plasmon resonance biosensor. Opt Commun 396:36–43
57. Pal S, Alka verma, Raikwar S, Prajapati YK, Saini JP, (2018) Detection of DNA hybridization using graphene-coated black phosphorus surface plasmon resonance sensor. Appl Phys A 124(5):1–11
58. Alagdar M, Nehal BY, Elzalabani F AM (2019) Improved the quality factor and sensitivity of a surface plasmon resonance sensor with transition metal dichalcogenide 2D nanomaterials. J Nanopart Res 22:189